Stability Analysis of a New Control Scheme for a Three-degree-of-freedom Flexible Arm under Tip Payload Changes

J.A. Somolinos*, V. Feliu and A. García.

Departamento de Ingeniería Eléctrica, Electrónica y Automática
E.T.S. de Ingenieros Industriales. U.C.L.M.
Campus Universitario s/n 13071 Ciudad Real, SPAIN

Abstract

This paper describes the stability analysis of a new control scheme for a three-degree-of-freedom flexible arm under tip payload changes. The arm was built with light links, has most of its mass concentrated at the tip, and uses a special mechanical configuration to approximately decouple radial tip motion from angular motions. This special configuration facilitates the modeling and control of the arm. A two nested loop controls the tip position. The value of the tip mass is used as a parameter to design the outer controller. Theoretical stability analysis of the controlled arm is carried out when tip mass differs from the mass used to design the outer loop. Experimental results are presented.

Keywords: flexible arms, robot control, computer control, stability analysis

1 Introduction

Traditionally, industrial robots have been designed and built in a manner that maximizes stiffness, in order to minimize vibration and allow for good positional accuracy with relatively simple controllers. The hypothesis of high stiffness links implies very inefficient arms because of their large weight compared to the mass they can handle. Flexible manipulators are proposed for applications where lightweight arms are required, like in aerospace industry, or robots to be mounted on mobile patforms,... If lightweight links are used to build robots, they become more flexible and more difficult to control accurately. Since the manipulator is a distributed dynamic system, the control difficulty is caused by the fact that a large number of oscillation are present into the dynamics of the arm.

We have built a spherical flexible arm of three degrees of freedom which is based on the next mechanical specifications:

*Corresponding Author. Tel.: 34 926 295300 extension 3812; Fax: 34 926 295361; e-mail: jasomol@ind-cr.uclm.es

1.- The arm must be lightweight (only tip mass is taken into account and any other masses are negligible)

2.- Radial motion of the tip has to be approximately kinematically decoupled from the angular motions if the arm is assumed rigid.

3.- It was wanted to build a flexible manipulator of similar features to a typical industrial robot as the $PUMA^{TM}$ six axes 560 robot (taken from [1]):

– Spherical volume with shoulder as center: 0.92 m.

– Maximum load: 2.3 kg including gripper.

– Tool acceleration/Tool velocity: 1.0 g max/1.0 m/s max.

The arm presented in this paper is light in weight in comparison with the mass placed at the tip because of the materials and dimensions of the links and because all the actuators are mounted at the base of the arm instead of placing an actuator at its elbow joint as in [2]. In this case, the flexible arms can be modeled as an structure where only one oscillation mode in each of the three orthogonal directions has to be considered. Then, the stiffness (or compliance) matrix and the tip mass are enough to characterize the oscillations of the structure from the expression $\omega_u^2 = \frac{k_u}{m}$, where m denotes the tip mass, k_u denotes the eigenvalues of the stiffness matrix, and ω_u denotes the tip vibration modes for u = 1,2 and 3. This very simple dynamic model of the arm with only one lumped mass is used to obtain a simple arm controller based on dynamics inversion of this model.

The tip controller is designed from the tip mass m_0, the compliance matrix $\mathbf{C}$ of the structure and the Jacobian of the rigid arm $\mathbf{J}$. $\mathbf{C}$ and $\mathbf{J}$ depend on the robot tip position.

The mass of the load that industrial robots handle usually changes with time. The influence of the tip mass into the dynamics of a flexible arm becomes very important with and without the arm controller. This paper presents the control scheme of a flexible arm of three degrees of freedom under nominal tip pay-

load, and the influence in the controlled arm of mass changes. Theoretical stability analysis of this control scheme based on Lyapunov's theorems [3, 4]is carried out under tip payload changes. Experimental results are presented.

Section 2 presents the control scheme under nominal payload conditions. The stability analysis of this control scheme is presented in Section 3 for the nominal tip mass, and in Section 4 for the case when the tip mass differs from the nominal mass. The experimental setup is briefly described in Section 5, experimental results that prove the previous theoretical analysis are exposed in Section 6, and conclusions are drawn in Section 7.

2 Control Scheme with Nominal Payload

The dynamics model of the proposed arm and the control scheme were presented in [5] and [6] respectively. Tip acceleration was used to control the arm instead of tip position measurements due to the large dimensions of the arm. Two kinds of sensors are used to control the arm: three encoders mounted on the motors give the motor position signals and three accelerometers attached at the arm tip give tip accelerations.

A two nested multivariable loop control structure is proposed. An inner loop is closed around the motors to control the joint angles, and then an outer loop is closed to control the tip position. The general scheme of this control structure is shown in Figure 1.

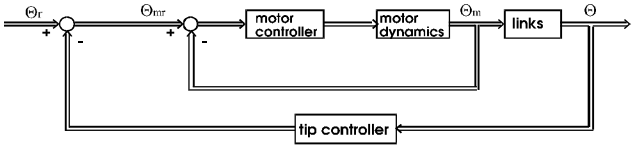

Figure 1: General Control Scheme

In Figure 1, $\mathbf{\Theta}_{mr} = \begin{pmatrix} \theta_{mr1} & \theta_{mr2} & \theta_{mr3} \end{pmatrix}^T$ denotes the motor angle references and $\mathbf{\Theta}_m = \begin{pmatrix} \theta_{m1} & \theta_{m2} & \theta_{m3} \end{pmatrix}^T$ represents the motor response of the three actuators. The inner loop is closed around the motors by using high gains controllers and feedforward compensation terms (a more detailed exposition can be seen in [6, 7]). Then the dynamics of the system becomes linear, and fast motor responses without any overshoot and with null steady-state errors are obtained.

The dynamics of the inner loop can be represented by a diagonal matrix of transfer functions between the motor references and the motor responses $\mathbf{\Phi}(s) = diag\{\mathbf{\Phi}_1(s)\ \mathbf{\Phi}_2(s)\ \mathbf{\Phi}_3(s)\}$. Then $\mathbf{\Theta}_m = \mathbf{\Phi}(s) \cdot \mathbf{\Theta}_{mr}$.

If very fast motor responses in comparison with the vibration frequencies of the arm are obtained, the dynamics of the inner loops can be neglected (as in [8, 9]), and then $\mathbf{\Phi}(s) \approx \mathbf{I}^{3\times 3}$ or $\mathbf{\Theta}_m \approx \mathbf{\Theta}_{mr}$. If the dynamics of the motors cannot be neglected, it is necessary to design a matrix of compensators $\mathbf{R}(s) = diag\{\mathbf{R}_1(s)\ \mathbf{R}_2(s)\ \mathbf{R}_3(s)\}$ located as shown in Figure 2, such that $\mathbf{R}(s) \approx \mathbf{\Phi}^{-1}(s)$ or $\mathbf{\Phi}(s) \cdot \mathbf{R}(s) \approx \mathbf{I}^{3\times 3}$. Then the expression $\mathbf{\Theta}_m = \mathbf{\Phi}(s) \cdot \mathbf{\Theta}_m$ becomes $\mathbf{\Theta}_m \approx \mathbf{\Theta}_{mr}$ as before. Saturation levels limit the validity of these compensators. Then, smooth trajectories have to be used in order to avoid this.

Figure 2 represents the dynamic model and control scheme of the arm in Cartesian coordinates [5, 6]. In our model, an infinitesimal friction term that represents any viscous friction has been added to fit the model responses with the real arm responses better. This friction term is represented by a diagonal positive definite matrix as:

$$\boldsymbol{\epsilon} = \begin{pmatrix} \epsilon_1 & 0 & 0 \\ 0 & \epsilon_2 & 0 \\ 0 & 0 & \epsilon_3 \end{pmatrix} \gtrapprox \mathbf{0}^{3\times 3} \tag{1}$$

From this equation and by using the Newton equation, the tip mass dynamics is:

$$\mathbf{F} = m_0 \cdot \ddot{\mathbf{P}} + \boldsymbol{\epsilon} \cdot \dot{\mathbf{P}}. \tag{2}$$

where $\mathbf{F}$ denotes the tip forces, m_0 denotes the nominal tip mass and $\mathbf{P}$ denotes tip position both in cartesian coordinates.

Let us define the stiffness matrix of the flexible structure as $\mathbf{C}^{-1}$ ($\mathbf{C}$ is the compliance matrix), and the Jacobian of the rigid arm $\mathbf{J}$, depending both of them on the tip position. Consider the manipulator whose dynamics is given by Figure 2

$$\mathbf{F} = \mathbf{C}(\mathbf{P})^{-1} \cdot \mathbf{J}(\mathbf{P}) \cdot [\mathbf{\Theta}_{mr} - \mathbf{\Theta}] \tag{3}$$

and controlled with the proposed control law [6]:

$$\mathbf{\Theta}_{mr} = \mathbf{\Theta}_r + \mathbf{J}(\mathbf{P})^{-1} \cdot \mathbf{C}(\mathbf{P}) \cdot m_0 \cdot \ddot{\mathbf{P}} \tag{4}$$

Substituting the control law (4) into the manipulator dynamic equation (3), yields

$$\mathbf{F} = \mathbf{C}(\mathbf{P})^{-1} \cdot \mathbf{J}(\mathbf{P}) \cdot \left[\mathbf{\Theta}_r + \mathbf{J}(\mathbf{P})^{-1} \cdot \mathbf{C}(\mathbf{P}) \cdot m_0 \cdot \ddot{\mathbf{P}} - \mathbf{\Theta}\right] \tag{5}$$

Eliminating $\mathbf{F}$ from equations (5) and (2) yields

$$\begin{aligned} m_0 \cdot \ddot{\mathbf{P}} + \boldsymbol{\epsilon} \cdot \dot{\mathbf{P}} = \\ = \mathbf{C}(\mathbf{P})^{-1} \cdot \mathbf{J}(\mathbf{P}) \cdot [\mathbf{\Theta}_r - \mathbf{\Theta}] + \\ + \mathbf{C}(\mathbf{P})^{-1} \cdot \mathbf{J}(\mathbf{P}) \cdot \mathbf{J}(\mathbf{P})^{-1} \cdot \mathbf{C}(\mathbf{P}) \cdot m_0 \cdot \ddot{\mathbf{P}} \end{aligned} \tag{6}$$

that can be simplified as

$$\boldsymbol{\epsilon} \cdot \dot{\mathbf{P}} = \mathbf{C}(\mathbf{P})^{-1} \cdot \mathbf{J}(\mathbf{P}) \cdot [\mathbf{\Theta}_r - \mathbf{\Theta}] \tag{7}$$

If small errors between the reference input and the tip response are considered, and denoting the error signal $\mathbf{E} = \mathbf{P}_r - \mathbf{P}$ as the difference between the equivalent Cartesian reference input and the real tip position in Cartesian coordinates, it can be obtained

$$\mathbf{J}(\mathbf{P}) \cdot [\mathbf{\Theta}_r - \mathbf{\Theta}] = \mathbf{P}_r - \mathbf{P} = \mathbf{E} \tag{8}$$

And then, equation (7) is transformed into

$$\boldsymbol{\epsilon} \cdot \dot{\mathbf{P}} = \mathbf{C}(\mathbf{P})^{-1} \cdot [\mathbf{P}_r - \mathbf{P}] = \mathbf{C}(\mathbf{P})^{-1} \cdot \mathbf{E} \qquad (9)$$

From the value of the friction matrix $\boldsymbol{\epsilon} \approx \mathbf{0}^{3\times3}$ and from the previous equation it can be obtained that

$$\mathbf{0}^{3\times3} \approx \mathbf{C}(\mathbf{P})^{-1} \cdot \mathbf{E} \qquad (10)$$

$$\mathbf{P}_r \approx \mathbf{P} \qquad (11)$$

Then, the tip follows the reference if equation (4) is used as control law.

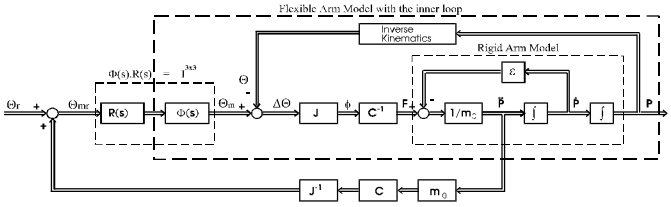

Figure 2: Control Scheme in Cartesian coordinates with friction

3 Stability Analysis with Nominal Payload

In this section, the stability of the control law proposed at Section 2 is proved. For only one degree of freedom systems, whose dynamics can be expressed in terms of Laplace transforms (at least at the neighbouhood of an equilibrium point), it is easy to determine the stability of the control algorithms by analyzing the poles and zeros location of the obtained transfer function. When more complex nonlinear systems of several degrees of freedom are used, the known stability Lyapunov's method and the asymptotic stability Lyapunov's method are used to prove the stability of a system [10],[3].

For proving the closed loop system stability, it is necessary to define a Lyapunov function. Consider the candidate Lyapunov function:

$$v = \frac{1}{2}\mathbf{E}^T \cdot \mathbf{E} \geq 0 \qquad (12)$$

which is always positive or zero because of its quadratic form, and verifies that is zero if and only if $\mathbf{E} = 0$, *i.e.* if $\mathbf{P}_r = \mathbf{P}$. Differentiating v with respect to time, results in

$$\frac{dv}{dt} = -\dot{\mathbf{P}}^T \cdot \mathbf{E} \qquad (13)$$

The error $\mathbf{E}$ is obtained from equation (9)

$$\mathbf{E} = \mathbf{C}(\mathbf{P}) \cdot \boldsymbol{\epsilon} \cdot \dot{\mathbf{P}} \qquad (14)$$

which substituted in equation (13) it gives

$$\frac{dv}{dt} = -\dot{\mathbf{P}}^T \cdot \mathbf{C}(\mathbf{P}) \cdot \boldsymbol{\epsilon} \cdot \dot{\mathbf{P}} \qquad (15)$$

Stiffness matrix $\mathbf{C}^{-1}$ and compliance matrix $\mathbf{C}$ are both symmetrical and positive definite. Then equation (15) is non positive and, using Lyapunov's theorem, the proposed control law implies global stability.

Moreover, taking $\mathbf{P}$ out of an arbitrarily small spherical region (or ball) of the reference position (case of $\|\mathbf{P}_r - \mathbf{P}\| \geq \alpha$), conditions of the Lyapunov asymptotical stability theorem are fulfilled and the control law (4) applied to the system (3) achieves global asymptotic stability.

It can be observed that if a null friction is supposed, ($\boldsymbol{\epsilon} = \mathbf{0}^{3\times3}$) the obtained derivative of the Lyapunov function $\frac{dv}{dt} = 0$ and the global stability theorem conditions are achieved but not the global asymptotic stability theorem conditions.

4 Stability Analysis with Non-Nominal Payload

The Lyapunov stability and asymptotic stability theorems have been already used in section 3. Here we use these theorems together with the Chetáev instability theorem to analyze the tip mass variation effect on the proposed control loop.

Figure 3 shows the case in which the tip mass m differs from the nominal mass m_0 used in the design of the control loop. It can be seen that this Figure is a generalization of Figure 2 for the case in which $m \neq m_0$.

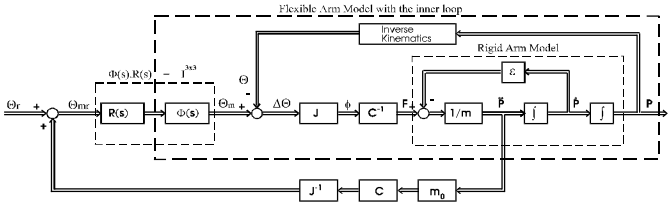

Figure 3: Dynamic model for the closed loop system whose tip mass m differs from the nominal m_0

If we consider an equilibrium point for the constant tip position $\mathbf{P}_r$, then the matrix $\mathbf{C}$ and the inverse Jacobian $\mathbf{J}^{-1}$ can be assumed constant for the neighbourhood of this equilibrium point. In this case, the system dynamics and its control law are obtained according to Figure 3:

$$\mathbf{F} = \mathbf{C}^{-1} \cdot \mathbf{J} \cdot [\boldsymbol{\Theta}_{mr} - \boldsymbol{\Theta}] \qquad (16)$$

$$\boldsymbol{\Theta}_{mr} = \boldsymbol{\Theta}_r + \mathbf{J}^{-1} \cdot \mathbf{C} \cdot m_0 \cdot \ddot{\mathbf{P}} \qquad (17)$$

Replacing control law (17) obtained for the nominal mass m_0 into the system dynamics (16) we get

$$\mathbf{F} = \mathbf{C}^{-1} \cdot \mathbf{J} \cdot \left[\boldsymbol{\Theta}_r + \mathbf{J}^{-1} \cdot \mathbf{C} \cdot m_0 \cdot \ddot{\mathbf{P}} - \boldsymbol{\Theta}\right]. \qquad (18)$$

Removing $\mathbf{F}$ from equations (18) and (2) it is obtained

$$m \cdot \ddot{\mathbf{P}} + \boldsymbol{\epsilon} \cdot \dot{\mathbf{P}} = \\ = \mathbf{C}^{-1} \cdot \mathbf{J} \cdot [\boldsymbol{\Theta}_r - \boldsymbol{\Theta}] + \mathbf{C}^{-1} \cdot \mathbf{J} \cdot \mathbf{J}^{-1} \cdot \mathbf{C} \cdot m_0 \cdot \ddot{\mathbf{P}} \tag{19}$$

that can be simplified as

$$(m - m_0) \cdot \ddot{\mathbf{P}} + \boldsymbol{\epsilon} \cdot \dot{\mathbf{P}} = \mathbf{C}^{-1} \cdot \mathbf{J} \cdot [\boldsymbol{\Theta}_r - \boldsymbol{\Theta}] \tag{20}$$

Assuming small errors between the tip position and its reference in joints coordinates, it is verified that

$$\mathbf{J} \cdot [\boldsymbol{\Theta}_r - \boldsymbol{\Theta}] = [\mathbf{P}_r - \mathbf{P}] \tag{21}$$

And equation (20) becomes

$$(m - m_0) \cdot \ddot{\mathbf{P}} + \boldsymbol{\epsilon} \cdot \dot{\mathbf{P}} = \mathbf{C}^{-1} \cdot [\mathbf{P}_r - \mathbf{P}] = \mathbf{C}^{-1} \cdot \mathbf{E} \tag{22}$$

Reorganizing and taking into account the meaning of $\mathbf{E} = \mathbf{P}_r - \mathbf{P}$, it easily follows:

$$(m - m_0) \cdot \ddot{\mathbf{P}} = -\boldsymbol{\epsilon} \cdot \dot{\mathbf{P}} + \mathbf{C}^{-1} \cdot \mathbf{E} \tag{23}$$

Case 1 $m > m_0$

Consider the following Lyapunov function:

$$v = \frac{1}{2} \cdot \dot{\mathbf{P}}^T \cdot (m - m_0) \cdot \dot{\mathbf{P}} + \frac{1}{2} \cdot \mathbf{E}^T \cdot \mathbf{C}^{-1} \cdot \mathbf{E} \geq 0 \tag{24}$$

This function remains positive or zero for any value of $\mathbf{P}$ and $\dot{\mathbf{P}}$ because the difference $(m - m_0)$ remains positive and the stiffness matrix $\mathbf{C}^{-1}$ is positive definite, being $v = 0$ if and only if $\mathbf{E} = 0$ and $\dot{\mathbf{P}} = 0$.

Differentiating v with respect to time results in

$$\frac{dv}{dt} = \dot{\mathbf{P}}^T \cdot (m - m_0) \cdot \ddot{\mathbf{P}} - \dot{\mathbf{P}}^T \cdot \mathbf{C}^{-1} \cdot \mathbf{E} \tag{25}$$

Multiplying equation (23) for $\dot{\mathbf{P}}^T$ and replacing in equation (25) yields

$$\frac{dv}{dt} = -\dot{\mathbf{P}}^T \cdot \boldsymbol{\epsilon} \cdot \dot{\mathbf{P}} + \dot{\mathbf{P}}^T \cdot \mathbf{C}^{-1} \cdot \mathbf{E} - \dot{\mathbf{P}}^T \cdot \mathbf{C}^{-1} \cdot \mathbf{E} \tag{26}$$

$$\frac{dv}{dt} = -\dot{\mathbf{P}}^T \cdot \boldsymbol{\epsilon} \cdot \dot{\mathbf{P}} \tag{27}$$

which is non positive, and the conditions of the Lyapunov asymptotic stability theorem are verified.

Therefore, the proposed control algorithm remains stable when the tip mass becomes larger than the nominal one that was used in the control design. On the other hand, when the tip mass becomes smaller than the nominal we can make the following analysis.

Case 2 $m < m_0$

Let us consider now the following Lyapunov function:

$$v = -\frac{1}{2} \cdot \dot{\mathbf{P}}^T \cdot (m - m_0) \cdot \dot{\mathbf{P}} + \frac{1}{2} \cdot \mathbf{E}^T \cdot \mathbf{C}^{-1} \cdot \mathbf{E} \tag{28}$$

This function remains positive or zero for any value of $\mathbf{P}$ and $\dot{\mathbf{P}}$ as the difference $(m - m_0)$ remains negative and the $\mathbf{C}^{-1}$ matrix is positive definite. Furthermore the function is derivable, and in any small neiborhood of the equilibrium point ($\mathbf{P} \neq \mathbf{P}_r$ or $\dot{\mathbf{P}} \neq 0$), there exists a region $v > 0$ in whose border ($\mathbf{P} = \mathbf{P}_r$ and $\dot{\mathbf{P}} = 0$) is $v = 0$.

Differentiating that equation with respect to time we get

$$\frac{dv}{dt} = -\dot{\mathbf{P}}^T \cdot (m - m_0) \cdot \ddot{\mathbf{P}} - \dot{\mathbf{P}}^T \cdot \mathbf{C}^{-1} \cdot \mathbf{E} \tag{29}$$

Multiplying equation (23) for $\dot{\mathbf{P}}^T$ and replacing it in equation (29) easily follows

$$\frac{dv}{dt} = \dot{\mathbf{P}}^T \cdot \boldsymbol{\epsilon} \cdot \dot{\mathbf{P}} + \dot{\mathbf{P}}^T \cdot \mathbf{C}^{-1} \cdot \mathbf{E} - \dot{\mathbf{P}}^T \cdot \mathbf{C}^{-1} \cdot \mathbf{E} \tag{30}$$

$$\frac{dv}{dt} = \dot{\mathbf{P}}^T \cdot \boldsymbol{\epsilon} \cdot \dot{\mathbf{P}} \tag{31}$$

which is positive for the region $v > 0$, that is to say, for $\mathbf{P} \neq \mathbf{P}_r$ or $\dot{\mathbf{P}} \neq 0$.

Furthermore, for any point $\dot{\mathbf{P}} \neq 0$ in which $v \geq \alpha > 0$ then $\frac{dv}{dt} \geq \beta > 0$. Therefore under the $m < m_0$ hypothesis, the conditions of the Chetáev instability theorem are verified. This means that, as the system becomes unstable in the neighbourhood of the equilibrium point $\mathbf{P}_r$, the system is unstable [3].

5 Experimental Setup

In this section, the experimental setup of the three-degree-of-freedom four-bar-linkage flexible arm is described.

The experimental arm was built to enable real-time control experiments. The mechanical system was designed to closely approximate the behavior of the ideal system, i.e., the arm is lightweight, carries an effective point mass at its tip, and has minimal friction and backlash. The arm was constructed from tubular aluminum bars (with an inner diameter of 13 mm and an outer diameter of 16 mm) and has a total mass of about 0.315 kg. The tip mass is a pair of disks that can be modeled as a point mass. Experimental results confirm this assumption. Tip mass can be adjusted using different disks, but it is typically 1.815 kg. Thus, the tip mass is substantially greater than the arm mass and, hence, the ratio of payload to robot weight is about 5.76 and, a lumped-mass model is reasonably assumed.

Figure 4: Overview of the real arm

Three passive joints connect the bars to get the mechanism. Figure 4 shows the real mechanism. Joint actuators are three brushless motors coupled with Harmonic Drive reduction gears. The three joints are situated on the base of the robot in order to minimize the inertia and mass of the arm. One servoamplifier powered by a common power supply is used for each motor. Two kinds of sensors are used to control the system. Three absolute encoders are used to measure the angular position of the three motors. Three accelerometers, attached to the tip, and arranged orthogonally, are used to sense the linear tip accelerations. The output analog signals of the accelerometers are amplified and filtered through in-line amplifiers. The outputs from the optical encoders are sent through three RS-422 lines, the acceleration data are sent to the computer through an A/D converter, and motor control signals are obtained from the computer through a D/A converter. A sampling period of T = 2 ms was chosen for the experiments (see [7]).

6 Experimental Results

The previous stability theoretical analysis of the control scheme is proved here in an experimental way. Three experiments are presented in this section: first, the plots included in Figure 5 show the tip acceleration response a_x with the complete controller and in the case that the outer loop has been removed, when an impulse motor position reference for the first actuator is applied in order to excite the structure at position $\mathbf{P}_r = \begin{bmatrix} x = 50.0 \text{ cm} & y = 0.0 \text{ cm} & z = 0.0 \text{ cm} \end{bmatrix}$ with $m = m_0$. We made the feedback outer controller act after t = 1 s. The tip acceleration responses a_y and a_z are not plotted here.

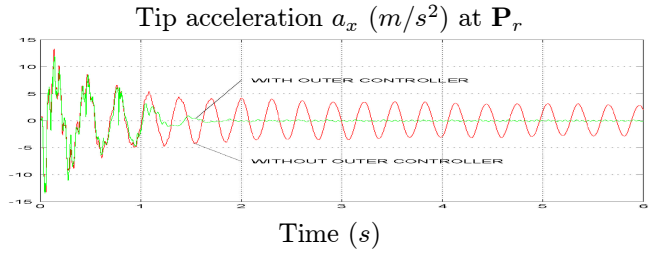

Figure 5: Tip acceleration a_x with and without the outer controller for $\mathbf{P}_r$

Secondly, Figure 6 shows the tip acceleration responses when the arm is with nominal payload ($m = m_0$) at the same point $\mathbf{P}_r$, and an external perturbation is produced knocking the tip three times. The time instants when the tip perturbation signals are produced can be clearly observed. The arm cancels the tip vibrations and restores the tip position $\mathbf{P}$ to $\mathbf{P}_r$ quickly.

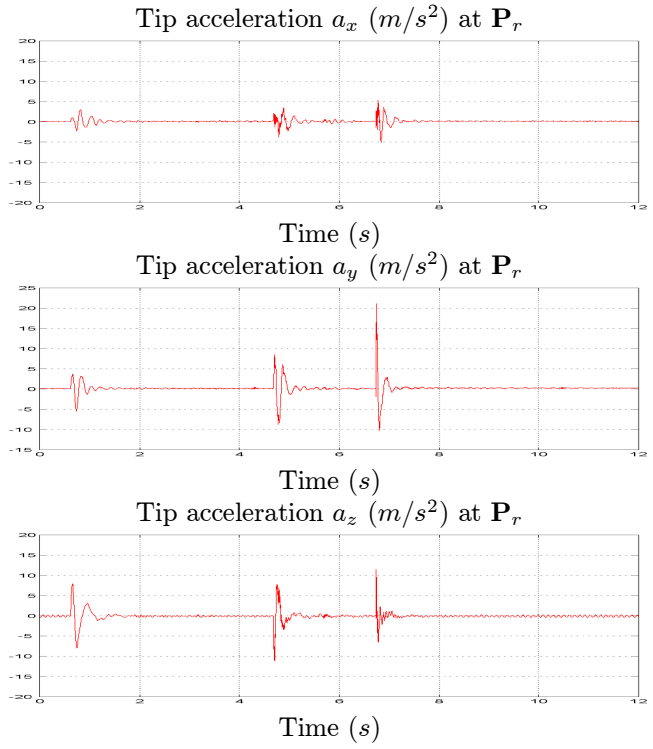

Figure 6: Tip acceleration response in the presence of external perturbations

Finally, the third experiment was carried out in the same tip position $\mathbf{P}_r$ and it can be resumed as follow:

1. Excite the structure with the inner control loop connected at t = 0 s with an impulse reference signal at the first joint, under nominal payload ($m = m_0$)

2. Connect the outer controller at t = 1 s.

3. Observe that tip oscillations have been removed.

4. Take out a disk of the tip mass. Then $m < m_0$ as in **Case 2**.

5. Produce a perturbation knocking the tip.

6. Disconnect the outer controller at t = 5 s.

Figure 7 shows this experiment. The experiment has been carried out with a tip mass of $m = 1.815$ kg which is changed to $m = 1.315$ kg. The tip acceleration signal a_x of this experiment is ploted in this Figure. Two vertical lines included in Figure 7 represent the instants when the outer controller is connected, and when the external perturbation is produced (steps *2* and *5*). It can be clearly observed the instability of the system under the condition of tip mass smaller than the nominal.

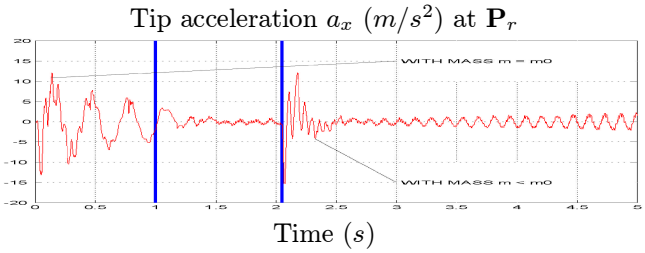

Figure 7: Tip acceleration a_x with nominal mass ($m = m_0$) and non nominal mass ($m < m_0$) for $\mathbf{P}_r$

7 Conclusions

The stability analysis of a new control scheme for a three-degree-of-freedom flexible arm has been presented in this paper. We have designed and controlled a new flexible manipulator with very simple dynamics in order to simplify the model and facilitate its control. The flexible arm is based on a special mechanism that shows some advantages to model and control the arm: it can be regarded as if all its mass were concentrated at its tip. Then a simple lumped masses model with only one mass at the tip is enough to characterize the dynamics of the flexible structure and only one oscillation mode in each of the three orthogonal directions is present, not being necessary the use of complex distributed masses models. Very simple control laws can be deduced from the proposed model. One control scheme based on tip acceleration feedback and dynamics inversion has been presented, which was designed for a nominal tip mass. The stability analysis of this control scheme has been carried out for nominal tip mass and for non nominal tip mass using the Lyapunov and Chetáev theorems.

From the obtained results, we can conclude that the proposed control algorithm is globally and asymptotically stable, and it remains stable when the tip mass becomes larger than the nominal mass and becomes unstable in the opposite case.

From this analysis it can be foreseen the interest of developing new adaptive or robust control schemes for flexible arms whose tip mass changes. These are the object of our current research.

8 Acknowledgments

This work has been supported by the Spanish CICYT under grant TAP-96-1028-C02-01.

References

[1] Unimation (Europe) Ltd., *Technical Documentation PUMA MK2 SYSTEM*, 1990.

[2] T. Yoshikawa, H. Murakami, and K. Hosoda, "Modeling and control of a three degree of freedom manipulator with two flexible links," in *Proceedings of the 1990 IEEE International Conference on Decision and Control*, (Honolulu, Hawaii), pp. 2532–2537, December 1990.

[3] J. E. Slotine and W. Li, *Applied Nonlinear Control*. Prentice Hall, 1991.

[4] L. Elsgoltz, *Ecuaciones diferenciales y cálculo variacional*. Editorial MIR Moscú, 3rd ed., 1983.

[5] J. Somolinos, V. Feliu, L. Sánchez, and J. Cerrada, "Design and experimental validation of a new three-degree-of-freedom flexible arm with simplyfied dynamics," in *XIV IFAC World Congress*, vol. B, (Beijing, China), pp. 101 – 106, July 1999.

[6] J. Somolinos, V. Feliu, L. Sánchez, and J. Cerrada, "Modeling and control of a new three-degree-of-freedom flexible arm with simplyfied dynamics," in *Proceedings of the 1999 IEEE International Conference on Robotics and Automation*, (Detroit, Michigan), pp. 435–440, May 1999.

[7] J. A. Somolinos, *Modelado dinámico y control de un robot flexible de tres grados de libertad*. PhD thesis, E.T.S. de Ingenieros Industriales. U.N.E.D., 1999.

[8] V. Feliu, K. S. Rattan, and H. Benjamin Brown, Jr., "Control of flexible arms with friction in the joints," *IEEE Transactions on Robotics and Automation*, vol. 9, pp. 467–475, August 1993.

[9] V. Feliu, K. S. Rattan, and H. Benjamin Brown, Jr., "Control of a two-degree-of–freedom lightweight flexible arm with friction in the joints," *Journal of Robotic Systems*, vol. 12, pp. 1–33, January 1995.

[10] J. J. Craig, *Introduction to Robotics. Mechanics and Control*. Addison-Wesley, 2nd ed., 1989.